From oil to microparticulate by prilling technique: production of polynucleate alginate beads loading *Serenoa Repens* oil as intestinal delivery systems

Angela Assunta Lopedota[a,*] Ilaria Arduino[a], Antonio Lopalco[a], Rosa Maria Iacobazzi[b], Annalisa Cutrignelli[a] , Valentino Laquintana[a], Giuseppe Racaniello[a], Massimo Franco[a], Flavia la Forgia[c], Sergio Fontana[c], Nunzio Denora[a,*]

[a] Department of Pharmacy – Pharmaceutical Sciences, University of Bari "Aldo Moro", Via E. Orabona, 4, I-70125 Bari, Italy
[b] IRCCS Istituto Tumori "Giovanni Paolo II", Via O. Flacco, Bari, Italy
[c] Centro Studi e Ricerche "Dr. S. Fontana 1900-1982", Farmalabor s.r.l., Via Piano S. Giovanni, 47, I-76012 Canosa di Puglia (BT), Italy

*** Corresponding authors:**
Department of Pharmacy – Pharmaceutical Sciences, University of Bari "Aldo Moro", Orabona St. 4, I-70125 Bari, Italy
E-mail addresses: nunzio.denora@uniba.it (Prof. N. Denora); angelaassunta.lopedota@uniba.it (Prof. A. Lopedota)

Abstract

Natural oils that are rich in biologically active polyunsaturated fatty acids have many health benefits, but have insufficient bioavailability and may oxidize in the gastrointestinal tract. For these reasons and to improve the handling as well, the possibility of incorporating a natural oil, extracted from *Serenoa Repens* fruits (SR-oil), in alginate-based beads was investigated. SR-oil has been used from centuries in both traditional and modern medicine for various nutraceutical or therapeutic purposes such as, in both sexes, as a general tonic, for genitourinary problems, to increase sexual vigor, as a diuretic or to treat in male lower urinary tract symptoms and benign prostatic hyperplasia. In this study, alginate-based beads prepared by vibration technology, also known as prilling technique, were explored as SR-oil delivery systems. Twenty-seven different formulations (P1-P27) were produced starting from stable emulsions at the period of the production. The formulations having spheroid shape (sfericity factor < 0.07), high preparation yield (> 90%) and high encapsulation efficiency (EE% > 80) were selected for further characterizations. Gas chromatographic analysis revealed a high loading of lauric acid as principal component of SR-oil allowing to calculate the content of total fatty acids (> 50%) into the beads. Swelling behavior and release features were also studied at different pH values. The swelling of the beads and their SR-oil release were negligible for the first 2 hours in simulated gastric fluid (pH 1.2), and appreciable in simulated intestinal fluid (pH 6.8).The release data were fitted by various equations to define the release kinetic mechanism. In addition, the selected formulation (P16) was stable to the oxidation not only during the preparation process, but also after 3 months of storage at room temperature. In summary, these polynucleate alginate beads produced by prilling technique, are promising systems for improving the intestinal specific delivery and bioavailability of health-promoting bioactive SR-oil.

Keywords*:* Serenoa Repens, alginate beads, microparticles, prilling, vibrating technology, intestinal drug delivery, benign prostatic hyperplasia.

1. Introduction

Saw palmetto (*Serenoa Repens*) is a small palm tree, native to South Eastern North America, particularly Florida. For many centuries saw palmetto berries were eaten by Native Americans and in the 20th century neuropathic doctors in the US began to recommend a tea made from its fruits as a diuretic and for the treatment of genitourinary problems. In the 1960's in Europe researchers led to the identification of the oil extracted from *Serenoa Repens* fruits (SR-oil) and its therapeutically active components, including free fatty acids (about 85%) or esterified fatty acids and sterols (Marti et al. 2019) (Edwards et al. 2015). Specifically, the main free fatty acids are: lauric (about 30%), oleic (about 30%) myristic (about 10%) and palmitic (about 10%) acids (Marti et al. 2019). At the present SR-oil is used for several nutraceutical or therapeutic purposes such as the treatment, in male, of the lower urinary tract symptoms and to reduce symptoms of benign prostatic hyperplasia (BPH). BPH is a widespread disease that affects the male population whose incidence is very difficult to identify. This pathology causes a non-malignant enlargement of the prostate, which can induce obstruction and inflammation of the lower urinary tract symptoms (LUTS) (Geavlete, Multescu, and Geavlete 2011). There are different pharmacological properties attributed to SR-oil such as anti-inflammatory and anti-androgen, but in the specific case of BPH, SR-oil can induce the inhibition of 5 α-reductase activity, which is involved in the pathological process of prostate enlargement (Fagelman and Lowe 2001). SR extract is commercially available as an oil, a powder through adsorption on maltodextrins and in pharmaceutical/nutraceutical grade as soft gelatin capsules, but still some disadvantages have been highlighted. In particular, the problems are the difficult handling and easy oxidation of the oil, the relative low quantity of SR-oil adsorbed on the maltodextrins and the possible detrimental effect in the stomach when SR-oil is released from the capsules.

In order to improve the handling of the SR-oil, it is recommended the conversion of the substance in a powder or microparticulate. In this regard, an innovative technique to transform liquid substances into solids is the realization of microparticle systems (Martins et al. 2017). The encapsulation of a substance, an oil in this case, is a process that allows to load an active ingredient in a polymeric matrix, which in turn can also provide its controlled delivery (Martins et al. 2017). Several techniques are used for microencapsulation including spray drying (Lopedota et al. 2016; Denora et al. 2016), fluid bed coating, spray cooling, melt injection and coacervation (Auriemma et al. 2020; Yilmaztekin et al. 2019). Basically, the choice of the process depends on the evaluation of a series of factors that includes the physical-chemical characteristics of the encapsulating/encapsulated materials, the size and structure of the microparticulate (matrix or reservoir), the achievement of

industrial scale up and economic issues (Martins et al. 2017). In this work, vibration technology better known as prilling or laminar jet breakup has been used as technique of microencapsulation. It is based on a mechanical process that allows to obtain different type of beads in a narrow dimensional range, high encapsulation efficiency and able to preserve the chemical stability of the loaded substance (Lopalco et al. 2020). . REF

Several types of polymers can be used for the development of beads, but the use of natural polymers is advantageous because of their biodegradability, biocompatibility and nontoxicity (Martău, Mihai, and Vodnar 2019). Among them, alginate is a naturally occurring anionic polysaccharide commonly used to prepare capsule or bead encapsulation systems due to its interesting physical-chemical properties, biocompatibility, wide availability and low cost (Lee and Mooney 2012; Martău, Mihai, and Vodnar 2019). For alginate, consolidation is achieved by ionotropic gelification in the presence of bivalent cations that may be Ca^{2+} or Zn^{2+}. Namely, when the alginate falls into the gelling solution, the polymer is immediately cross-linked by ion exchange (Azad et al. 2020; Lee and Mooney 2012). Calcium alginate beads possess hydrogel properties that could control release at intestinal level, transiting unaltered through the stomach, and the mucoadhesive properties could improve their residence on the intestinal mucosa (Azad et al. 2020).

The overall aim of this study was to encapsulate high content of SR-oil in calcium-alginate beads by emulsion/prilling technique. Initially, stability studies were carried out to establish the best emulsions suitable for the prilling process. Subsequently, different beads were prepared and characterized. For the best beads formulation, swelling and release studies were performed in simulated gastric and intestinal fluids. Moreover, the release data were fitted to various equations to determine the release kinetic mechanism.

2. Materials and Methods

2.1. Materials

Serenoa Repens liposoluble extract obtained by supercritical CO_2 extraction from ripe fruits of Serenoa repens and sodium alginate, manuronic and guluronic acids ratio (M/G), : 1.8-2.2; viscosity 500-600 mPa*s (sol 1%) were gifted by Farmalabor srl, Canosa di Puglia, Italy. Calcium chloride dihydrate, polysorbate 80, Hydranal® KF reagent, lauric acid, sodium thiosulfate ($Na_2S_2O_3$), potassium hydroxide (KOH), potassium iodide (KI) and iodine bromide solution were purchased from Sigma Aldrich (Milan, Italy). All solvents and salts used were of analytical grade and purchased from Sigma Aldrich.

2.2. Preparation of SR-oil/alginate emulsion

Sodium alginate powder was dispersed in distilled water to produce alginate solutions of desired concentrations (0.5%, 1%, 1.5%, 2% and 2.5% w/v) using a high shear mixer (Ultra-Turrax T25, Janke e Kunkel, Germany) at 13200 rpm for 3 minutes. Five emulsions were prepared, between alginate solutions and SR-oil (7% v/v) using a high shear mixer at 13200 rpm for 5 minutes (Table S1).

2.3. Stability of emulsion

In order to evaluate creaming and/or phase separation phenomena, the stability at 25°C of the emulsions, after 1 and 24 hours from their preparations, was assessed by visual analysis, optical microscopy and Static Multiple Light Scattering. The visual analysis of the emulsions stability was reported as ES percentage (Eq. 1) where V_{emul} and $V_{initial}$ were the volume occupied from emulsion in the cylinder after 1 and 24 hours and zero time respectively (Huang, Kakuda, and Cui 2001).

$$ES\ (\%) = \frac{V\ emul}{V\ initial} \times 100 \quad (1)$$

For the microscopic analysis, a Leica III Optical Microscope was used, equipped with a Panasonic camera (WV CP 230), which mounts an image analysis program (Leica Qwin 2.4 software). The mean diameter value of SR-oil droplets was calculated for each emulsion at 0, 1 and 24 hours.

Physical stability measurements of the oil droplets were conducted, by Static Multiple Light Scattering using the Turbiscan Lab® Expert (Formulaction, France). In detail, each sample (20 mL) was pipetted into flat-bottomed cylindrical glass tubes, placed into the instrument and kept for 4 hours, at 25 °C. This instrument permits to reveal premature instability of emulsion because, even though, an emulsion appears homogeneous to a naked eye, it may just have phenomena of instability. The apparatus was composed of a pulsed near infrared light source (wavelength 880 nm) and two synchronized detectors, which were used to collect the transmitted lights and backscattering lights. The detectors scanned the entire length of the tube to acquire transmission flux and backscattering flux every 40 μm. The obtained data were expressed as a percentage intensity of the transmission or backscattering since the emulsions were opaque the backscattering intensity was used to evaluate the destabilization status. Furthermore, the global total scattering index (TSI) value developed by Turbiscan® was considered. The TSI is a single value metric (0-10 or more) that corresponds to a cumulative sum of all the backscattering and transmission across the entire sample based on specific algorithm. Essentially, lower is the number, more stable is the sample.

2.4. Preparation of sodium alginate beads loading SR-oil

Nine alginate-oil emulsions were prepared, considering a sodium alginate concentration of 1%, 2% and 2.5% w/v, and 3%, 5% and 7% w/v of SR-oil (Table S2). With the aim to set up the production of beads with desired properties, the 9 different emulsions were processed by Prilling instrument (Encapsulator B-395 Pro, Büchi Labortechnik AG, Switzerland) at the flow rate of 1, 4 and 7.5 mL/min, obtaining 27 different beads formulations (Table 1). The other parameters of the instrument were fixed, namely, the alginate-oil emulsions were pumped using a syringe pump through a 750-micron nozzle, the vibration frequency set to break up the laminar liquid jet was 450 Hz and the electrode potential was 1000V. The distance between the vibrating nozzle and the gelling bath was fixed at 20 cm.

Table 1. Combination of the 27 different formulations (P1 – P27) obtained by varying the sodium alginate, SR-oil concentrations and the flow rate.

	Flow rate (mL/min)								
	1	4	7.5	1	4	7.5	1	4	7.5
Sodium Alginate (% w/v)	**Formulation**								
1	P1	P2	P3	P4	P5	P6	P7	P8	P9
2	P10	P11	P12	P13	P14	P15	P16	P17	P18
2.5	P19	P20	P21	P22	P23	P24	P25	P26	P27
	SR-oil (% w/v)								
	3			5			7		

Gelling solution consisted of a 0.1 M $CaCl_2$ and 1% w/v Tween 80 aqueous solutions gently stirred in which the emulsion droplets were consolidated and held for 15 minutes. Then the obtained beads were separated from the gelling solution by filtration using paper filters and washed with bidistilled water for two times before dried. Two methods were used for drying the beads, specifically by static oven and by freeze drying. Concerning the first method (oven), the prepared beads were placed on a paper filter of known weight and then in a stove (WTB Binder) at 30 °C, until constant weight was reached. In the second method (lio), the beads were placed on a paper filter of known weight, frozen at -20 °C and then dried by freeze-drying technique for 24 h using a Christ Alpha 1–4 LSC under reduced pressure (0.018 mbar) at -50 ° C.

2.5. Sphericity factor of beads

The size and the shape of the beads before drying were determined using an image analyzer (Sigma ScanPro 5). A digital camera was used to capture the images of the wet beads. Sphericity factor

(SF) was used to indicate the roundness of the beads, as described by Chan et al. (2009), where the value zero indicates a perfect sphere and higher values indicate a greater degree of shape distortion (Azad et al. 2020). SF was calculated according to Equation 2:

$$SF = \frac{D0-D90}{D0+D90} \quad (2)$$

where D_0 is the maximum diameter passing through a bead centroid (mm) and D_{90} is the diameter perpendicular to D_0 passing through the bead centroid (mm).

2.6. Beads size

The size of spheroid beads (formulations P1-P10, P13 and P16) was measured directly for wet beads by a digital caliper (TEKNA PRO) and by optical microscopy for dried beads. For each batch, a minimum of fifty beads were examined to evaluate the mean diameter and their relative standard deviations. The reduction in the beads size after drying was expressed by the shrinkage factor (SrF) and calculated according to the Equation 3.

$$SrF = \frac{D\,wet-Ddry}{Dwet} \quad (3)$$

2.7. Determination of encapsulation efficiency and production yield

The encapsulation efficiency percentage (EE%) of the lio and oven dried beads was determined by indirect method (Chan 2011) (Eq. 4 and 5 respectively).

$$EE\ (\%) = \frac{W_2}{W_1} \times 100 \quad (4)$$

$$EE\ (\%) = \frac{W_3}{W_1} \times 100 \quad (5)$$

Where W_1 is the initial amount of SR-oil used and W_2 is W_1 subtracted of the amount of SR-oil left on the paper filter during drying.

For oven dried beads, because of the presence of oil on their surface, it was necessary to wash the beads for 2 minutes with ethyl acetate. For this reason, W_3 is W_1 subtracted of both the amounts of SR-oil left on the paper filter and the SR-oil eliminated by washing.

The percentage yield (Y%) of the process was calculated as ratio between the weight of harvested beads and the total weight of alginate and used SR-oil (Eq. 6).

$$Y\ (\%) = \frac{g\ microbeads}{g\ (Alginate+\ SR-oil)} \times 100 \quad (6)$$

2.8. Karl Fischer Titration

The water content of the beads was quantified by Karl Fischer (KF) titration using a C30S Mettler Toledo. In particular, the formulations analysed were P10, P13 and P16. Approximately 100 mg of beads were dissolved in anhydrous methanol. The resulting solution was injected into the KF reaction cell filled with Hydranal® KF reagent and then the amount of water was examined. Pure solvent was also injected for use as a background sample.

2.9. Lauric acid content determination

Ten milligrams of the dried beads were disintegrated in 10 mL of phosphate buffer (pH 6.8) in 3 hours, then SR-oil was extracted with 10 mL of ethyl acetate, and the organic phase was separated from aqueous phase by centrifugation. The organic phase was analysed to determine the content of lauric acid by Agilent Technologies 7890A GC gas chromatograph fitted with an Agilent J&W 30 m X 0.25 µm capillary column, with hydrogen as the carrier gas (constant flow rate of 20 mL min^{-1}) and flame ionization detector (FID). The temperature program was: 70 °C for 2 min and up to 250 °C (20 °C per minute). The temperature of the injector and the detector were maintained during the analysis at 260 and 300 °C respectively. The calibration curve was obtained using 5 standard lauric acid solutions which were analysed under the same condition as the samples.

2.10. Bead Swelling Behaviour

The swelling behaviour of the dried beads was evaluated by gravimetric method. Exactly weighed aliquots of P16 formulations (oven and lio) were placed inside a cylinder with a square mesh base and a known tare. The swelling experiments were carried out at a temperature of 37 °C , dipping the cylinder for 2 hours in the fluid simulating the gastric environment (SGF) at pH 1.2 and then in phosphate buffer simulating the intestinal environment (SIF) at pH 6.8 until their disintegration (Yotsuyanagi et al. 1987; Yotsuyanagi et al. 1991). At regular intervals of 15 min the cylinder containing the sample was lightly dried and weighed. The degree of swelling (Sw) was calculated as the weight ratio between the final weight of the re-hydrated beads (wf) and their initial weight (wi) (Eq 7).

$$Sw = \frac{wf}{wi} \tag{7}$$

2.11. Drug release and kinetic studies

Release studies were conducted using the Agilent 708DS 8 Position Dissolution System. The rotational speed of the rotating basket was set at 75 rpm and the temperature of the dissolution medium was maintained at 37 °C. For each experiment, a quantity of beads equivalent to 320 mg of SR-oil was weighed and subsequently poured into 800 mL of SGF for 2 hours and then in SIF for others 3 hours. At set times and after a strong stirring of the dissolution medium, withdrawals of 5 mL were made and replaced with an equal volume of fresh medium. The collected samples were extracted using ethyl acetate and analysed for the content of lauric acid as described above. The amount of the SR-oil released during the time was calculated considering that about 30% of 93% of total fatty acid in SR-oil was lauric acid. The dissolution profile was obtained by plotting the cumulative percentage of SR-oil released on the y-axis and time (in minutes) on the x-axis.

In the present study, raw data obtained from in vitro release studies were fitted by different release kinetic equations including zero-order (Cumulative percentage drug released versus time), first-order (Log cumulative percentage drug remaining versus time) Higuchi model (Cumulative percentage drug released versus square root of time) and Korsmeyer–Peppas model (Log cumulative percentage drug remaining versus log time) (Baishya 2017).

2.12. Oxidative stability of the SR-oil in the beads

The iodine value (I_I) was assessed according to the Ph.Eu. (Method A, 01/2008:20504) [Ph. Eur. 6.0, 2008]. To determine I_I, 0.2 g of SR-oil (extracted from an appropriate amount of beads by following the method described in paragraph 2.9) was dissolved in hexane. At this organic solution were added first 20 mL of 0.2 N iodine bromide solution and, after 30 minutes, 10 mL of 10% KI solution at room temperature and in the dark condition. Then, the reaction mixture was diluted with 100 mL of water and titrated with a 0.1 N solution of $Na_2S_2O_3$ under stirring. A fresh 1% starch solution was used as reaction indicator and a blank sample was titrated under the same conditions. The results were expressed as g of I_2 / 100 g of extract oil.

The peroxide value (I_p) was assessed according to the Ph.Eu. (Method A, 01/2008:20505) [Ph. Eur. 6.0, 2008]. To determine I_p, 2.0 of extracted SR-oil from the beads was dissolved in 30 mL of a mixture of chloroform (2v) and acetic acid (3v). At this reaction mixture, were added 0.5 mL of saturated KI solution and after 30 min, 30 mL of deionized water. The final reaction mixture was titrated with 0.01N solution of $Na_2S_2O_3$ under magnetic stirring. A fresh 1% starch solution was used as reaction indicator, and a blank sample was titrated under the same conditions. The results were expressed as meqO_2 / kg of extract oil.

The oxidative stability of SR-oil was evaluated for hydrated beads (P16) and dried beads (lio- and

oven P16) and finally, on lio P16 after 3 months of storage in glass vial with screw cap at room temperature.

2.13. Statistical analysis

The experimental data were reported as mean ± SD (standard deviation). Statistical analysis was conducted by Graph Prism version 6.0 (Graphad Sofware Inc., La Jolla, CA, USA).

3. Results and Discussions

This study was aimed to develop polynucleate alginate beads as innovative intestinal SR-oil delivery systems, capable to increase the bioavailability of its biologically active polyunsaturated fatty acids by protecting them from oxidation. As first step, a stable O/W emulsion was identified to facilitate the process adopted for the preparation of the microbeads, namely the prilling technique. Twenty-seven different microbeads were prepared and characterized to select the ones with suitable properties. Furthermore, the formulation that allowed both to release mainly at intestinal pH value and to increase oxidation stability of the SR-oil was identified.

3.1. Stability of SR-oil/alginate emulsions

The first step of the SR-oil encapsulation procedure was the preparation of O/W emulsions obtained emulsifying SR-oil (7% v/v) in an sodium alginate aqueous solution (0.5, 1, 1.5,2 and 2.5% w/v). Concentration of sodium alginate higher than 2.5% w/v was not considered since its aqueous solution was too viscous for the process (Kaushik and Roos 2007). The homogenizator Ultraturrax was chosen to obtain stable O/W emulsions with fine internal oil droplets. Indeed this process was quicker (5 minutes) than a mechanical stirrer (45 minutes), as already reported (Chan et al. 2011).

For our aim, the stability of emulsion, without modification of internal size oil droplets, have to be maintained before and during the encapsulation process since a stable emulsion has a substantial influence on the encapsulation efficiency and on final characteristics of the product (Gharsallaoui et al. 2007; Klaypradit and Huang 2008; Tan, Chan, and Heng 2005). The most common initial sign of instability of O/W emulsion is a creaming and may then be followed by coalescence of oil droplets within the cream (where an oil layer is formed at the top of emulsion). Creaming as well as sedimentation are two results of gravitational forces, and they are often the result of a difference in densities between the dispersed phase (oil) and the continuous phase (water) (Hu et al. 2017).

In this study, five emulsions, named S1-S5 (Table S1), were estimated about stability by different methodologies such as visual inspection, optical microscopy and static multiple light scattering.

3.1.1. Visual inspection and optical microscopy

The visual inspection, as emulsion stability percentage (ES%), was carried out after 1- and 24-hours preparation, in order to assess short- and long-term stability, for both small- and large-scale production. In detail, except for emulsion P1 (85%), after 1 h of storage a good physical stability was calculated for emulsions S2-S5 indicating that concentrations of sodium alginate ≤ 0.5% w/v were not suitable to guarantee a prolonged stability. Even though, this phenomenon depends from the type of used alginate and its properties such as molecular weight, ratio M/G etc. (Chan et al. 2011). The ES%, after 24 h, for S1-S5 O/W emulsions are shown in Figure S1. This value is higher, about 100% when alginate concentration increased, as observed for the emulsions S4 and S5. The emulsions were also observed using an optical microscopy to estimate the increment of oil droplet size. The starting emulsion presented a reduction of SR-oil droplet dimensions as alginate concentration increased (1.5±0.30, 1.41±0.46, 1.25±0.50, 1.15±0.57 and 0.95±0.23 μm from S1 to S5, respectively), reducing the potential creaming/sedimentation instability phenomena of emulsions as indicated from Stokes' law (Spasic 2018).

After 1 h, for all emulsions a little increase (about 10%) of oil droplet size was observed (1.7±0.3, 1.65±0.52, 1.45±0.35, 1.22±0.30 and 1.05±0.26 μm). Instead, after 24 h, the oil droplet size for E1 and S2 were about 300% bigger (4.80±0.82 and 4.65±1.26 μm, respectively) than initial preparation suggesting a possible coalescence of internal phase. The oil droplet size observed for S3, S4 and S5 increased only of about 60% with the best performance for S4. This major stability registered may be due to an increment in viscosity of the continuous phase surrounding the oil droplets restricting their movement (Huang, Kakuda, and Cui 2001). Some representative images of oil droplets, after 1 and 24 hours from preparation, are showed in Figure 1.

<<Insert Figure 1>>

3.1.2. Static multiple light scattering

Based on previous results, the emulsions that provided the worst and the best stability (S2 and S4, respectively) were studied using Turbiscan® Lab Expert. In Figure 2, are presented the backscattering graphs for tested samples during a period of 4 hours. In particular, panel A1 highlights an increment in backscattering intensity from 35 to 62% on the top (height 32.0–42.0 mm) of tube containing the sample S2, which indicates a creaming process occurring during the analysis. ~~This took place when the water content at the top of the emulsion reduced and oil gradually separated from the emulsion.~~ Similarly, the backscattering decreases from 35 to 5 % on the bottom and center (height 0.2–32 mm) of the tube, suggesting a clarification process, which

occurs when oil droplets in emulsion gradually coalesced and settled to the top, while the water phase migrated towards the bottom of the sample.

Destabilization of an emulsion has been shown to be accompanied by two phenomena: droplet size variation (aggregation, coalescence) and droplet migration (creaming, clarification) (Buron et al. 2004). The former is irreversible, and the latter is reversible under mechanical agitation. Considering the studies of optical microscopy and static multiple light scattering**,** S2 was identified as an irreversible emulsion, in the 4 hours (Figure 2, panel A1). On the contrary, the emulsion S4 was stable without important changes, with a backscattering passing from 47 to 43% in the same time of investigation (Figure 2, panel B1). This minimum variation of backscattering in all length of the sample could indicate an increment of size of dispersed phase with possible initial flocculation.

Furthermore, the global total scattering index (TSI) value developed by Turbiscan® was equal to 23 and 3.4 for S2 and S4, respectively (Figure 2, panels A2 and B2). The TSI can be used to compare and rank stability, hence, also this parameter confirmed that S4 was stable while S2 was strongly unstable after 4 hours. However, the emulsion S2 could be used if it is immediately processed within 40 minutes….E

<<Insert Figure 2>>

3.2. Manufacturing of SR oil-loaded beads

The choice of the technology more appropriate for SR-oil encapsulation was based on an intricate balance between productivity, cost, encapsulating material and chosen dimension of the beads. Alginate beads were produced by Encapsulator B-395 Pro by vibrations (prilling) technology inducing ionotropic gelling of the drops of the emulsion SR-oil/sodium alginate aqueous solution with $CaCl_2$ (Del Gaudio et al. 2015). Droplets generation by the vibration technology was achieved applying vibrations on the emulsion laminar fluid jet, which broke apart definitely if the right wavelength was applied. The bead size was adjusted mainly by the nozzle diameter and the wavelength although also other parameters, e.g. viscosity, influenced the droplets formation (Heinzen, Berger, and Marison 2004). Twenty-seven preparations, code P1-P27 (Table 1) were designed starting from 9 emulsions obtained varying the concentration of sodium alginate and SR-oil (Table S2). Then, each emulsion was prilled with three different flows, 1, 4 and 7.5 mL/min. The wet beads obtained were firstly characterized about shape and size, then splitted in two parts and dried by thermal (oven beads) or freeze-drying (lio beads) methods.

3.3. Shape of wet beads

Using a digital camera, the images of the wet beads were photographed and according to SF, as above described, the roundness of beads was calculated. A value zero indicates a perfect sphere and higher values indicate a greater degree of shape distortion (Azad et al. 2020). Spheres were realized with preparations at 1% w/v of alginate (P1-P9) independently from the flow, and 2% w/v of alginate (P10, P13 and P16) when the flow rate was set at 1 mL/min (Figure 3). To maintain the droplet shape, a good balance of forces such as viscosity, surface tension of emulsion, and the impact-drag of the droplets on the surface of consolidation bath have be considered. It was demonstrated that SR-oil emulsions at alginate concentration < 1% w/v were insufficient to obtain beads because the characteristics of this emulsion did not counteract the effect of impact and drag in gelling bath. Beads were obtained, between 1 and 2% w/v alginate of SR-oil emulsions, beads were obtained but in according with literature, the extrusion of high viscosity polymer solutions (i.e. high concentration polymer solutions) gave deformed particles having shape of eggs or elongated beads (see Figure 3) (Levic et al. 2013; Prüsse et al. 2008). Finally, with alginate concentration > 2.5% w/v the emulsion was too viscous to permit the formation of droplets from the nozzle. These data permitted to focus the study on spherical beads since are more convenient than irregular ones. Indeed, spherical beads have a low surface/volume ratio, producing a lower diffusion of oil in the beads. Furthermore, spherical wet beads are more prone to realize spherical dried beads that could to have a better flow influencing the repartition in dosage form as capsules, sachets, tablets etc. For further analysis, starting from the 27 designed and prepared formulation it was selected only the realized spheroid beads (code P1-P10, P13 and P16).

<<Insert Figure 3>>

3.4. Diameter of beads

In Table S3, the diameter of beads, measured in mm, are presented. The wet beads range from 1.49 to 2.69 mm, that is about two or three times the diameter of the nozzle used in the process (0.750 mm).

With vibrating jet technique, the jet was break-up in homogeneous droplets due to asymmetric disturbances caused by vibration. The size of droplets depended essentially on the nozzle diameter and the fluid properties (viscosity, density and surface tension). Therefore, the final size and shape of the beads was influenced by forming droplets at the jet nozzle but also by it's the shirking in the gelation/consolidation phase of the droplets.

The beads were dried by two different apparatus: freeze dryer (lio) and oven. A slight reduction in size of the lio-dried beads was measured contrary to the oven-dried beads, as the shrinkage factors

(SrF) revealed (Table S3). Probably, during the drying, the frozen matrix of the beads did not collapse, permitting to have similar wet bead sizes. This is typical for a freeze-dried product where the original frozen volume is generally maintained. The table also shows that the SrF is correlated to alginate concentration, but not to amount of SR-oil loaded into the beads. Final wet and dried beads are presented in Figure 4. Some differences for the beads were evident for the lio-dried ones. The beads' surface was light green and not oily unless a greater force was applied to squeeze the oil out from the beads. Probably, the surface and internal pores acted as small capillaries, allowing absorbing and holding the SR-oil like a reservoir. On the contrary, the oven-dried beads were dark green less spherical, aggregate and oily on the surface. During this drying, the shrinkage of the beads pushed out part of SR-oil loaded on the surface facilitating probably the oxidation of some component of SR-oil.

<<Insert Figure 4>>

3.5. Yield of process and encapsulation efficiency

The yield of the process for the dried beads selected (P1-P10, P13 and P16) was calculated as percentage in weight between the harvested beads and the amount of alginate and SR-oil used for each batch. On average, the percentage of yield was quite high (> 65%). Low yields can be attributed to a combination of factors such as the dissipation of emulsion during the emulsification process, the loss of SR-oil both in the reticulation bath, and, above all, during the drying.

The oven-dried beads had a range of yield 65-90%, with lower values for P1-P9. Probably, the alginate 1% w/v had a matrix not enough robust to retain the entrapped SR-oil when the beads shrinked during drying. The lio-dried beads had same rank yield P1-P9 < P10, P13, P16, but higher values (87-98%) than oven-beads.

The encapsulation efficiency percentage (EE%) is the ratio between the quantity of oil present in the beads compared to oil loaded. The SR-oil encapsulated in the matrix was calculated indirectly considering the amount of oil lost during the process. The data of EE% for dried beads are presented in table 2. Generally, it was found that drying in oven caused the leak of SR-oil from the wet beads and this explained the low EE% values. Particularly, this phenomenon was prevalent for the beads formed with alginate 1% w/v. In contrast, for lio beads there was negligible free oil on the beads' surface as confirmed by high EE% and no detection of residual SR-oil on the papers during the drying. From these results, it was concluded that the formulations at 2% w/v of alginate (P10, P13 and P16) were the best as efficiency encapsulation. Indeed, a minimum SR-oil was lost during the preparation of the beads, and considering SR-oil is expensive, it is advisable to have higher

EE% than loading (see table 2). In added, considering the typical dosage of SR-oil equal to 0.320 g the quantity of the P10, P13 and P16 beads ranges in acceptable unit dose (0.537, 0.478 and 0.418 g). This advantage combined with other favorable quality reported above, elected them as candidate formulations.

Table 2. Encapsulation of efficiency and loading of oven- and lio-dried beads*. The value is the mean of three determinations and deviation standard relative was < of 10%** g SR-oil per g of beads

Code Formulation	EE* (%) Oven-dried	Loading**	EE* (%) Lio-dried	Loading**
P1	72.2	0.684	95.1	0.740
P2	75.2	0.699	88.3	0.720
P3	73.4	0.687	90.5	0.731
P4	69.4	0.776	91.8	0.803
P5	65.6	0.766	92.8	0.823
P6	62.8	0.758	89.8	0.818
P7	64.8	0.819	89.0	0.862
P8	61.7	0.811	87.7	0.860
P9	60.3	0.808	83.8	0.854
P10	88.0	0.569	98.0	0.595
P13	84.0	0.677	92.0	0.697
P16	83.4	0.745	93.7	0.766

3.6. Karl Fisher titration and total fatty acids titration

Karl Fisher titration is an accurate method for water determination from few ppm to near saturation in a sample. We applied this test at the three selected dried beads (P10, P13 and P16) in order to evaluate the efficiency of drying. The residual water in the beads was low and a slight difference was present between the drying methods adopted. The lio-dried beads had a percentage of water higher than oven-dried ones as showed in table 3. This difference could depend on the nature of lio-dried beads, that, being amorphous and porous, were capable of retaining greater amount of water. By means an extractive and a quantitative GC method, the total fatty acids in the beads were calculated. The lauric acid was identified as principal component (about 30%) of total fatty acids SR-oil that were the 93% w/w of all SR-oil (as technical datasheet reported). The identification of the lauric acid peak was achieved by retention time, comparing it with the standards analyzed under the same conditions. After quantitative analysis of the lauric acid in the beads, it was converted, by calculation, in total fatty acids (Table 3). The best formulation was the P16 obtained with the maximum amount of SR-oil loaded (7% v/v), where the highest amount of fatty acid was encapsulated (69.3%). This is an important result reached, because a typical commercial spray dried

powder based on maltodextrin loads about of 45% of total fatty acid. This goal was also realized, but to a lesser extent, with P10 and P13, hence, for the following studies, it was decided to use only the best P16 both oven and lio.

Table 3. Value of water (moisture) from dry beads using Karl Fisher titration. Lauric acid determined by GC and total fatty acid in 100 g of formulation are mean of three determinations. ± is the deviation standard.

Formulation	Water %	Lauric acid %	Total Fatty acid %
oven P10	0.921±0.050	14.8±0.5	49.3
lio P10	6.371±0.210	15.5±1.5	51.6
oven P13	2.951±0.150	17.6±1.3	58.6
lio P13	2.033±0.162	19.0±0.9	63.3
oven P16	1.623±0.103	19.2±1.1	64.0
lio P16	2.089±0.120	20.8±1.4	69.3

3.7. Bead Swelling Behavior

Swelling of polymeric beads is a significant characteristic that influences the release pattern (Guru, Nayak, and Sahu 2012). The release of the encapsulated drug from the dried beads requires a re-hydration process of hydrophilic alginate that swells the dry beads for a difference in osmotic pressure of the fluid inside and outside the beads. In detail, swelling occurs in two steps that require the transport of water and Na^+ ions to gel beads by diffusion mechanism and the disintegration of gel caused by partial Na^+-Ca^{2+} ion exchange. Indeed, as the Ca^{2+} ions are exchanged, electrostatic repulsion between the carboxylate anions of alginic acid accelerates the swelling and erosion of alginate gel (Kikuchi et al. 1997). Moreover, upon ionization, the counter-ion concentration inside the polymeric network increases, and an osmotic pressure difference exists between the internal and external solutions of the beads (Soppimath, Kulkarni, and Aminabhavi 2001). The data of the swelling study obtained by gravimetric method of P16 (oven and lio) are presented in Figure 5.

<<Insert Figure 5>>

A linear profile was obtained in the SGF, but during the two hours of the study, the beads increased their weight only 2 and 3.6 times for oven and lio-dried respectively, without any sign of disintegration. When the beads were transferred from acid to basic environment an immediate (first 30 minutes) reduction of their weight was registered, probably caused by shrinkage of the polymeric structure due to a sudden change of pH. In the SIF the swelling of the particles took place

gradually up to a maximum weight at 180 minutes, after the beads disintegrated progressively until to disappear at 300 minutes. The exchange of calcium ions can be used to explain the swelling behavior of the beads in alkaline pH where the presence of calcium-sequestrant phosphate ions helped to bind the carboxylic groups of cross-linked alginate matrix and the sodium ions found in phosphate buffer. This caused turbidity in the phosphate buffer, as calcium phosphate was formed (Mallappa, Kesarla, and Banakar 2015). A little difference in swelling behavior was observed between the oven and lio beads, this last had a higher swelling probably due to more porosity of them thanks to drying process adopted. The particular features in the media for the studied beads suggest that the system can be used to convey SR-oil in intestinal direction and to obtain a modified release systems, in which the alginate carrier, directs the SR-oil to the first digestive tract releasing it slowly.

3.8. In vitro release and kinetic studies

Generally, an encapsulated drug is released from alginate beads because the dissolution medium penetrates into alginate beads and controls swelling and disintegration of alginate hydrogel. In the meantime, the encapsulated drug dissolves in the medium and subsequently leaks through the swollen hydrogel (Kikuchi et al. 1997; Soppimath, Kulkarni, and Aminabhavi 2001). As indicated above, and elsewhere (Wright et al. 2009), the alginate has a structural resistance to the acidic environment, but it is gradually disintegrated in the mild alkali condition. The drug release patterns of SR-oil loaded dried beads (oven and lio P16) in the SGF (pH 1.2) and SIF (pH 6.8) at 37 °C was shown in Figure 5 panel B. The cumulative percentage of SR-oil released in the SGF is significantly low compared to one in the SIF ($p < 0.05$). In detail, in the SGF medium, the beads released after two hours only 12.3 and 6% of SR-oil for lio and oven P16, respectively. This may be due to the stability and poor swelling property of alginate matrix in acidic medium (LEE, MIN, and CUI 1999) and the conversion of matrix Ca-alginate to insoluble alginic acid (Hodsdon et al. 1995).

The remaining SR-oil was gradually released in the SIF medium, during the subsequently three hours. Most of the SR-oil was released from the beads as the erosion rate in the SIF increased, confirming the hypothesis reported in the swelling study and suggesting that P16 can really be used as intestinal site-specific drug delivery system. Indeed, P16 had a pH-dependent drug release behavior that it is essential when the carrier travel across gastro-intestinal tract (Zeeb et al. 2015).

To define the drug release profile, several mathematical equations are available. Once an appropriate function has been selected the evaluation of drug release profile carried out can be correlated with drug release kinetic models (Baishya 2017). In this study, different release equation models were applied to understand the mechanism of SR-oil release from alginate beads. The

correlation coefficient (R2) slope, intercept and release exponent (n) values are reported in table S4. The highest degree of R2 determines the suitable mathematical model that follows drug release kinetic (Rescigno 2001). The correlation coefficient in the SGF were found to fit well (R2=0.98) with first order for lio P16, and with the zero-order kinetic or Hixson Crowell for oven P16. The diffusional or release exponent (n) values was 0.52 and 0.77, for lio and oven P16 respectively, indicating probably an anomalous transporter, non fickian diffusion. In the SIF, all the evaluated models fit well R2 > 0.94, but Higuchi drug release and Hixson Crowell model were the best (R2 0.98-0.99). Hence, the possible mechanism of SR-oil release was the diffusion controlled, and considering the Hixson Crowell model, the dissolution mechanism from the matrix beads have also be advocated. It describes as change in surface area and diameter of the beads is a function of time with a progressive dissolution of matrix. Besides, the diffusion exponent was superior to 0.89 for both lio and oven P16 which implied that the drug release from the system followed a super case transport (Banker, Slepman and Rhodes 2002). This release mechanism occurred through the polymer dissolution controlled and polymeric chain expansion or polymer relaxation/swelling.

3.9. Oxidative stability of SR-oil loaded in the beads

As reported in technical sheet, the used SR-oil extract is composed mainly of free fatty acids (93.5%) or esterified fatty acids (methyl-, ethyl-esters and triglycerides). The highest free fatty acids (express as percentage of free fatty acid compared to total fatty acids) are lauric (30.2%) and oleic (28.5%) acids followed by myristic, palmitic and linoleic acids. Since SR-oil contain a high concentration of unsaturated fatty acids (free and bound) such as oleic acid and linoleic acid (low amount), the peroxide index and the iodine number were used as parameters of the oxidative stability of the SR-oil loaded in the beads during the process (production and drying) and storage. The peroxide value is a function of fatty acids oxidation and the iodine value is indicative of the unaltered content of the unsaturated fatty acids.

The results obtained are reported in Table 4. The hydrate beads showed I_p and I_I values close to those of the pure SR-oil, and they increased slightly for lio dried beads. While the oven dried beads showed to be more sensitive to oxidation, since the oil leaked from the beads and surrounding the surface was more exposed to the air during drying (I_p =18.7 meqO_2/Kg). The I_I value, due to its high content of unsaturated fatty acids (both free and bound), ranged from 35.5 to 44.5 gI_2/100g proving the feasibility of the freeze-drying process compared to drying with heat. Therefore, in the evaluation of the long-term stability only the lio beads were stored. These exhibited a good stability of the encapsulated SR-oil after 3 months of storage.

Table 4: Peroxide value Ip and iodine value II of pure SR-oil, hydrate beads, lio and oven P16 beads and a sample of lio P16 after 3 months of storage.

Sample	I_p ($meqO_2/Kg$)	I_I ($gI_2/100g$)
Pure SR-oil	2.5±0.2	44.5±1.5
Oil extract from hydrate beads	2.8±0.2	43.2±0.8
Oil extract from lio P16	3.5±0.3	44.0±1.2
Oil extract from oven P16	18.7±0.8	35.5±1.0
Oil extract from lio P16 stored after 3 months	4.3±0.3	42.5±1.4

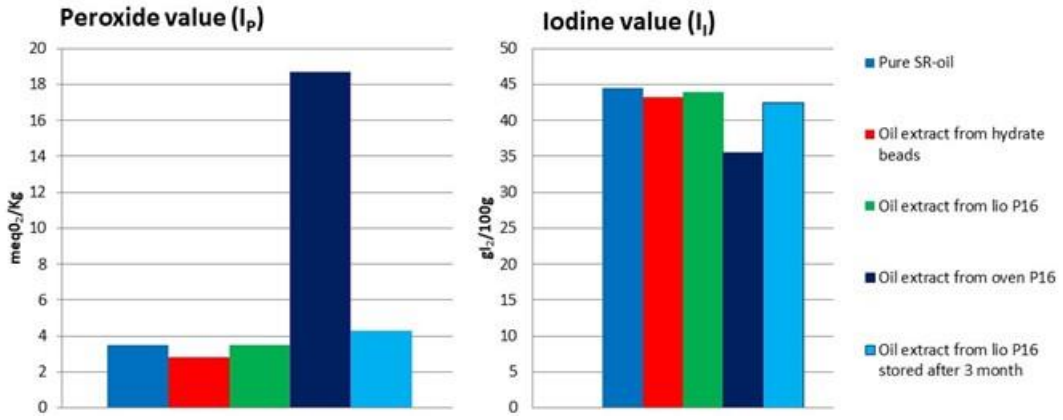

4. Conclusion

The present research proposed a novel formulation to encapsulate SR-oil in swellable hydrogel alginate beads, for intestinal site-specific drug delivery. SR is an oil present in pharmaceutical product and dietary supplement with different applications especially for BHP. The research project established a procedure for SR-oil encapsulation to turn the oil in microparticulate and to open the possibility for application of new SR-solid formulations. Different emulsions were prepared as starting material between SR-oil and aqueous alginate and the best emulsions were individuated after deep analysis. Starting from these emulsions, different formulations were designed and prepared and some were selected by several investigations such as size, shape, yield and encapsulation efficiency. The selected formulations were the ones with 2% (w/v) of sodium alginate with three different percentage of SR-oil loaded (3, 5 and 7% v/v). Further analysis permitted to individuate among the three formulation, the 7% v/v in SR-oil as the best and on this were carried out swelling and drug release studies. They revealed that the new drug delivery system studied could convey SR-oil more specifically to the intestine. Furthermore, the prilling method adopted was not detrimental for the SR-oil and its encapsulation help to reduce premature oxidation during the storage.

Aknowledgment

Authors acknowledge the University of Bari “Aldo Moro” (Italy) for its financial support with the project: “Fondi di Ateneo contributo ordinario di supporto alla ricerca 2017/2018”. This work was also partially supported by Fondazione Puglia (Italy) with the project: “Turbiscan lab expert”. Authors are greateful to Farmalabor S.r.l. for its technical support.

References

Auriemma, G., A. Cerciello, R. P. Aquino, P. D. Gaudio, B. M. Fusco, and P. Russo. 2020. 'Pectin and Zinc Alginate: The Right Inner/Outer Polymer Combination for Core-Shell Drug Delivery Systems', *Pharmaceutics*, 12.

Azad, A. K., S. M. A. Al-Mahmood, B. Chatterjee, W. M. A. Wan Sulaiman, T. M. Elsayed, and A. A. Doolaanea. 2020. 'Encapsulation of Black Seed Oil in Alginate Beads as a pH-Sensitive Carrier for Intestine-Targeted Drug Delivery: In Vitro, In Vivo and Ex Vivo Study', *Pharmaceutics*, 12.

Baishya, Himankar. 2017. 'Application of Mathematical Models in Drug Release Kinetics of Carbidopa and Levodopa ER Tablets', *Journal of Developing Drugs*, 06.

Buron, H, O Mengual, G Meunier, I Cayré, and P Snabre. 2004. 'Optical characterization of concentrated dispersions: applications to laboratory analyses and on-line process monitoring and control', *Polymer International*, 53: 1205-09.

Chan, Eng-Seng. 2011. 'Preparation of Ca-alginate beads containing high oil content: Influence of process variables on encapsulation efficiency and bead properties', *Carbohydrate Polymers*, 84: 1267-75.

Chan, Eng-Seng, Sze-Ling Wong, Peh-Phong Lee, Jau-Shya Lee, Tey Beng Ti, Zhibing Zhang, Denis Poncelet, Pogaku Ravindra, Soon-Hock Phan, and Zhi-Hui Yim. 2011. 'Effects of starch filler on the physical properties of lyophilized calcium–alginate beads and the viability of encapsulated cells', *Carbohydrate Polymers*, 83: 225-32.

Del Gaudio, Pasquale, Felicetta De Cicco, Francesca Sansone, Rita Patrizia Aquino, Renata Adami, Maurizio Ricci, and Stefano Giovagnoli. 2015. 'Alginate beads as a carrier for omeprazole/SBA-15 inclusion compound: A step towards the development of personalized paediatric dosage forms', *Carbohydrate Polymers*, 133: 464-72.

Denora, N., A. Lopedota, M. Perrone, V. Laquintana, R. M. Iacobazzi, A. Milella, E. Fanizza, N. Depalo, A. Cutrignelli, A. Lopalco, and M. Franco. 2016. 'Spray-dried mucoadhesives for

intravesical drug delivery using N-acetylcysteine- and glutathione-glycol chitosan conjugates', *Acta Biomater*, 43: 170-84.

Ph. Eur. 6.0, 137-138 (01/2008).

Fagelman, E., and F. C. Lowe. 2001. 'Saw Palmetto Berry as a Treatment for BPH', *Reviews in urology*, 3: 134-38.

Geavlete, P., R. Multescu, and B. Geavlete. 2011. 'Serenoa repens extract in the treatment of benign prostatic hyperplasia', *Ther Adv Urol*, 3: 193-8.

Gharsallaoui, Adem, Gaëlle Roudaut, Odile Chambin, Andrée Voilley, and Rémi Saurel. 2007. 'Applications of spray-drying in microencapsulation of food ingredients: An overview', *Food Research International*, 40: 1107-21.

Guru, Pravat, Amit Nayak, and Rajendra Sahu. 2012. 'Oil-entrapped sterculia gum-alginate buoyant systems of aceclofenac: Development and in vitro evaluation', *Colloids and surfaces. B, Biointerfaces*, 104C: 268-75.

Heinzen, Christoph, Andreas Berger, and Ian Marison. 2004. 'Use of Vibration Technology for Jet Break-Up for Encapsulation of Cells and Liquids in Monodisperse Microcapsules', *Fundamentals of Cell Immobilisation Biotechnology*, 8.

Hodsdon, Alison C., John R. Mitchell, Martyn C. Davies, and Colin D. Melia. 1995. 'Structure and behaviour in hydrophilic matrix sustained release dosage forms: 3. The influence of pH on the sustained-release performance and internal gel structure of sodium alginate matrices', *Journal of Controlled Release*, 33: 143-52.

Hu, Yin-Ting, Yuwen Ting, Jing-Yu Hu, and Shu-Chen Hsieh. 2017. 'Techniques and methods to study functional characteristics of emulsion systems', *Journal of Food and Drug Analysis*, 25: 16-26.

Huang, X., Y. Kakuda, and W. Cui. 2001. 'Hydrocolloids in emulsions: particle size distribution and interfacial activity', *Food Hydrocolloids*, 15: 533-42.

Kaushik, Vikas, and Yrjö Roos. 2007. 'Limonene encapsulation in freeze-drying of gum Arabic–sucrose–gelatin systems', *LWT - Food Science and Technology*, 40: 1381-91.

Kikuchi, Akihiko, Minako Kawabuchi, Masayasu Sugihara, Yasuhisa Sakurai, and Teruo Okano. 1997. 'Pulsed dextran release from calcium-alginate gel beads', *Journal of Controlled Release*, 47: 21-29.

Klaypradit, Wanwimol, and Yao-Wen Huang. 2008. 'Fish oil encapsulation with chitosan using ultrasonic atomizer', *LWT - Food Science and Technology*, 41: 1133-39.

LEE, BEOM-JIN, GEUN-HONG MIN, and JING-HAO CUI. 1999. 'Correlation of Drug Solubility with Trapping Efficiency and Release Characteristics of Alginate Beads', *Pharmacy and Pharmacology Communications*, 5: 85-89.

Lee, Kuen Yong, and David J. Mooney. 2012. 'Alginate: properties and biomedical applications', *Progress in polymer science*, 37: 106-26.

Levic, Steva, Verica Djordjevic, Nevenka Rajic, Milan Milivojevic, Branko Bugarski, and Viktor Nedovic. 2013. 'Entrapment of ethyl vanillin in calcium alginate and calcium alginate/poly(vinyl alcohol) beads', *Chemical Papers*, 67: 221-28.

Lopalco, A., N. Denora, V. Laquintana, A. Cutrignelli, M. Franco, M. Robota, N. Hauschildt, F. Mondelli, I. Arduino, and A. Lopedota. 2020. 'Taste masking of propranolol hydrochloride by microbeads of EUDRAGIT® E PO obtained with prilling technique for paediatric oral administration', *Int J Pharm*, 574: 118922.

Lopedota, A., A. Cutrignelli, V. Laquintana, N. Denora, R. M. Iacobazzi, M. Perrone, E. Fanizza, M. Mastrodonato, D. Mentino, A. Lopalco, N. Depalo, and M. Franco. 2016. 'Spray Dried Chitosan Microparticles for Intravesical Delivery of Celecoxib: Preparation and Characterization', *Pharm Res*, 33: 2195-208.

Mallappa, Manjanna Kolammanahalli, Rajesh Kesarla, and Shivakumar Banakar. 2015. 'Calcium Alginate-Neusilin US2 Nanocomposite Microbeads for Oral Sustained Drug Delivery of Poor Water Soluble Drug Aceclofenac Sodium', *Journal of drug delivery*, 2015: 826981-81.

Martău, Gheorghe Adrian, Mihaela Mihai, and Dan Cristian Vodnar. 2019. 'The Use of Chitosan, Alginate, and Pectin in the Biomedical and Food Sector-Biocompatibility, Bioadhesiveness, and Biodegradability', *Polymers*, 11: 1837.

Marti, Guillaume, Philippe Joulia, Aurélien Amiel, Bernard Fabre, Bruno David, Nicolas Fabre, and Christel Fiorini-Puybaret. 2019. 'Comparison of the Phytochemical Composition of Serenoa repens Extracts by a Multiplexed Metabolomic Approach', *Molecules (Basel, Switzerland)*, 24: 2208.

Martins, Evandro, Denis Poncelet, Ramila Rodrigues, and Denis Renard. 2017. 'Oil encapsulation techniques using alginate as encapsulating agent: applications and drawbacks', *J Microencapsul*, 34: 1-18.

Prüsse, Ulf, Luca Bilancetti, Marek Bučko, Branko Bugarski, Jozef Bukowski, Peter Gemeiner, Dorota Lewińska, Verica Manojlovic, Benjamin Massart, Claudio Nastruzzi, Viktor Nedovic, Denis Poncelet, Swen Siebenhaar, Lucien Tobler, Azzurra Tosi, Alica Vikartovská, and Klaus-Dieter Vorlop. 2008. 'Comparison of different technologies for alginate beads production', *Chemical Papers*, 62: 364.

Rescigno, Aldo. 2001. 'Foundations of pharmacokinetics', *Pharmacological research : the official journal of the Italian Pharmacological Society*, 42: 527-38.

Soppimath, Kumaresh S., Anandrao R. Kulkarni, and Tejraj M. Aminabhavi. 2001. 'Chemically modified polyacrylamide-g-guar gum-based crosslinked anionic microgels as pH-sensitive drug delivery systems: preparation and characterization', *Journal of Controlled Release*, 75: 331-45.

Spasic, Aleksandar M. 2018. 'Chapter 1 - Introduction.' in Aleksandar M. Spasic (ed.), *Interface Science and Technology* (Elsevier).

Tan, L. H., L. W. Chan, and P. W. Heng. 2005. 'Effect of oil loading on microspheres produced by spray drying', *J Microencapsul*, 22: 253-9.

Wright, Peter J., Elisabetta Ciampi, Caroline L. Hoad, Anthony C. Weaver, Michael van Ginkel, Luca Marciani, Penny Gowland, Michael F. Butler, and Phillippa Rayment. 2009. 'Investigation of alginate gel inhomogeneity in simulated gastro-intestinal conditions using magnetic resonance imaging and transmission electron microscopy', *Carbohydrate Polymers*, 77: 306-15.

Yilmaztekin, Murat, Steva Levic, Ana Kalušević, Mustafa Çam, Bugarski Branko, Vesna Rakić, Vladimir Pavlovic, and Viktor Nedović. 2019. 'Characterization of peppermint (Mentha piperita L.) essential oil encapsulates', *J Microencapsul*, 36: 1-30.

Yotsuyanagi, Toshihisa, Tsuneo Ohkubo, Takafumi Ohhashi, and K. E. N. Ikeda. 1987. 'Calcium-Induced Gelation of Alginic Acid and pH-Sensitive Reswelling of Dried Gels', *CHEMICAL & PHARMACEUTICAL BULLETIN*, 35: 1555-63.

Yotsuyanagi, Toshihisa, Isamu Yoshioka, Naoki Segi, and Ken Ikeda. 1991. 'Acid-Induced and Calcium-Induced Gelation of Alginic Acid : Bead Formation and pH-Dependent Swelling', *CHEMICAL & PHARMACEUTICAL BULLETIN*, 39: 1072-74.

Zeeb, Benjamin, Amir Hossein Saberi, Jochen Weiss, and David Julian McClements. 2015. 'Formation and characterization of filled hydrogel beads based on calcium alginate: Factors influencing nanoemulsion retention and release', *Food Hydrocolloids*, 50: 27-36.